Hindawi Publishing Corporation
Journal of Nanomaterials
Volume 2013, Article ID 137275, 8 pages
http://dx.doi.org/10.1155/2013/137275

Research Article

Synthesis and Magnetic Properties of a Superparamagnetic Nanocomposite "Pectin-Magnetite Nanocomposite"

Jude Namanga,[1] Josepha Foba,[2] Derek Tantoh Ndinteh,[3] Divine Mbom Yufanyi,[2] and Rui Werner Maçedo Krause[3]

[1] *Institute of Physics, Department of Chemical Physics and Material Science, University of Augsburg, 86153 Augsburg, Germany*
[2] *Department of Chemistry, Faculty of Science, University of Buea, P.O. Box 63, Buea, Cameroon*
[3] *Department of Chemistry, Rhodes University, Grahamstown 6140, South Africa*

Correspondence should be addressed to Josepha Foba; jnfoba@yahoo.com

Received 14 May 2013; Revised 27 July 2013; Accepted 12 August 2013

Academic Editor: Do Kim

Magnetic nanocomposites composed of superparamagnetic magnetite nanoparticles in a pectin matrix were synthesized by an in situ coprecipitation method. The pectin matrix acted as a stabilizer and size control host for the magnetite nanoparticles (MNPs) ensuring particle size homogeneity. The effects of the different reactant ratios and nanocomposite drying conditions on the magnetic properties were investigated. The nanocomposites were characterized by X-ray diffraction (XRD), scanning electron microscopy (SEM), transmission electron microscopy (TEM), energy dispersive X-ray spectroscopy (EDX), Fourier-transform infrared (FT-IR) spectroscopy, and superconducting quantum interference device magnetometer (SQUID). Superparamagnetic magnetite nanoparticles with mean diameters of 9 and 13 nm were obtained, and the freeze-dried nanocomposites had a saturation magnetization of 54 and 53 emu/g, respectively.

1. Introduction

Superparamagnetic nanocomposites are an important class of advanced materials with possible applications as magnetic drug carriers, hyperthermia local inductors for cancer therapy, magnetic cell separators, biological sensors, and magnetic resonance imaging [1–4]. For these applications, it is often necessary that the nanocomposites are biocompatible, nontoxic, and biodegradable [5]. Important developments have been reported in the synthesis of drug targeting delivery systems, in which particles of metal oxides (mostly maghemite, γ-Fe_2O_3, or magnetite, Fe_3O_4) are embedded in biocompatible and biodegradable polymeric matrices [6, 7]. For such practical uses of MNPs, the particle sizes, magnetic properties, and surface properties are of great importance. These properties are reported to be influenced by the synthesis method employed [8].

Magnetite nanoparticles with particle sizes less than 20 nm (less than the domain size for that material) are regarded as superparamagnetic as each particle is composed of a single magnetic domain [9]. Such superparamagnetic particles display a distinct magnetization curve with no coercive and remanent responses when placed in a magnetic field, a required and important magnetic property in most biomedical applications of magnetic particles [10, 11].

Typically, magnetisation values for superparamagnetic iron oxide nanoparticles (SPIONS) range from 30 to 50 emu/g, while higher values (e.g., 90 emu/g) have been observed for bulk materials [12]. Factors contributing to the magnetisation value of SPIONS include the size of the particles (with the highest emu/g to volume ratio occurring for particles in the 6–20 nm particle size range), the spacing between the nanoparticles (where coatings such as silica separate the magnetic domains, allowing each individual magnetite particle to act independently and thus enhancing the net magnetism per gram), and the crystalline structure of the iron oxide. It is therefore essential to use a method of SPION production that generates particles with one or more of the above characteristics [12].

In the coprecipitation synthesis there are two main processes involved. The first is a short single burst of nucleation, followed by growth of the nuclei. The precipitation

method provides an advantage because large quantities can be synthesised; however, problems arise from the wide particle size distribution [12, 13].

The coprecipitation method is simple, cost-effective, and the nanoparticles obtained are hydrophilic. The particle sizes are controlled by coating with pectin. The polysaccharide, pectin, is an inexpensive, nontoxic product extracted from citrus peels or apple pomace. Basically, it consists of a polymer of α-D-galacturonic-acid units with $1 \rightarrow 4$ linkages [12, 14].

In this paper we report an in situ coprecipitation approach for the synthesis of magnetite nanoparticles in a cheap polymer matrix (pectin). The effect of stoichiometric ratio of magnetite to pectin on the properties of the nanocomposites also presented. The important influence of the drying conditions (air- and freeze-drying) on the saturation magnetisation of the pectin-coated magnetite nanoparticles is highlighted.

2. Materials and Methods

2.1. Materials. Ferrous and ferric chloride (99.9% pure), pectin with degree of esterification of 76%, and ammonia solution were purchased from Sigma Aldrich. All the chemicals were of analytical grade and used without further purification. Distilled water purified through a Millipore system was used as the solvent.

2.2. Experimental. The required mass of pectin was dissolved in 200 mL of water under stirring. The reaction flask was degassed by the flow of nitrogen gas for 30 minutes and set under inert atmosphere. The appropriate masses of ferric and ferrous salts were dissolved each in 30 mL distilled water, degassed as above, and added to the pectin solution, which resulted in a brown gel. Water (40 mL) was used to transfer the remaining iron solutions, making a net volume of 300 mL. The masses used for each sample are shown in Table 1. The reaction solution was left under a gentle flow of nitrogen for a further 10 minutes, after which an excess of ammonium hydroxide (1.5 M) solution was added as the precipitating agent. The pH of the solution rose from 2.5 to 11, and the solution became black indicating the formation of magnetite. The nanocomposites were rinsed several times with distilled water until the pH dropped to approximately 7. Each sample was divided into two portions; one set was air-dried and the other set freeze-dried. The syntheses were conducted at room temperature.

2.2.1. Characterization. FTIR spectra of pectin and pectin-magnetite nanocomposites were recorded on a PerkinElmer Spectrum 100-FT-IR spectrometer from 400 to 4000 cm^{-1} at 10 scans per run. The crystallinity and phase purity of the nanocomposites formed were determined by powder X-ray diffraction (pXRD) on a Bruker D8 Advance Diffractometer using a CuKα radiation source (λ = 0.15406 nm, 40 kV and 40 mA). Scans were taken over the 2θ range from 10° to 80° in steps of 0.01° at room temperature using open quartz sample holders. The morphology of the nanocomposites was determined by scanning electron microscopy on Jeol-Jem 2100 electron microscope. Energy dispersive X-ray detector coupled to the SEM provided information on the chemical composition of the nanocomposites. Transition electron microscope (TEM) images were recorded on a Jeol JSM 7500F electron microscope. The particle size distributions were determined from the TEM images using the imageJ software.

The magnetic properties of the nanocomposites were measured by SQUID magnetometer on the powder samples. The saturation magnetisation was measured at variable magnetic field at a constant temperature of 300 K.

3. Results and Discussion

All four samples of PIO-1 and PIO-2 had an even black colour after drying, but the PIO-3 sample had a mixture of black particles with brown beads of varied sizes (the beads appeared to be poorly formed aggregates of iron-oxide clusters, and this sample was not further characterised).

3.1. Powder X-Ray Diffraction (XRD). Figure 1 shows the pXRD patterns of PIO-2 (blue, PIO-2A and PIO-2F) and PIO-1 (red, PIO-1A and PIO-1F) nanocomposites. The diffraction peaks indicating formation of other compounds are not observed. The diffraction patterns have well defined peaks and indicate that the samples are crystalline. The diffraction peaks are indexed as (220), (311), (400), (422), (440), and (511) crystal planes, corresponding to a cubic unit cell of magnetite [15], and they match the inverse-spinel structure of magnetite (space group of Fd3m, JCPDS Card no. 79 - 0417). The coprecipitation of maghemite is excluded by the absence of the (210) and the (110) peaks, which in the case of maghemite are present and at slightly higher intensities than the (111) peak. The diffraction peaks of PIO-2 are broader than those of PIO-1, indicating the finer nature and smaller crystallite sizes of the particles.

The average particle sizes were calculated using the Scherer equation [15]:

$$D_{hkl} = \frac{k\lambda}{b\cos\theta}, \tag{1}$$

where D_{hkl} is the average particle size; the equation uses the corrected reference peak width at angle θ. λ is the X-ray wavelength, b is the corrected width of the XRD peak at half height, and k is the shape factor, which is approximated as 0.9 for magnetite [15]. Interestingly, the particle sizes of PIO-1A and PIO-1F, PIO-2A and PIO-2F were found to be the same, meaning the drying conditions had no effect on the particle sizes. The calculated values are summarised in Table 2.

The inter-planer spacing (d_{hkl}) of the (311) diffraction was calculated using [16]

$$d_{hkl} = \frac{\lambda}{2\sin\theta}. \tag{2}$$

The calculated d_{hkl} values for PIO-1 and PIO-2 were found to be 2.533 Å and 2.528 Å, respectively. Comparing these values to the standard values for magnetite (2.532 Å; JCPDS no. 19-629) and maghemite (2.518 Å; JCPDS no. 39-1346),

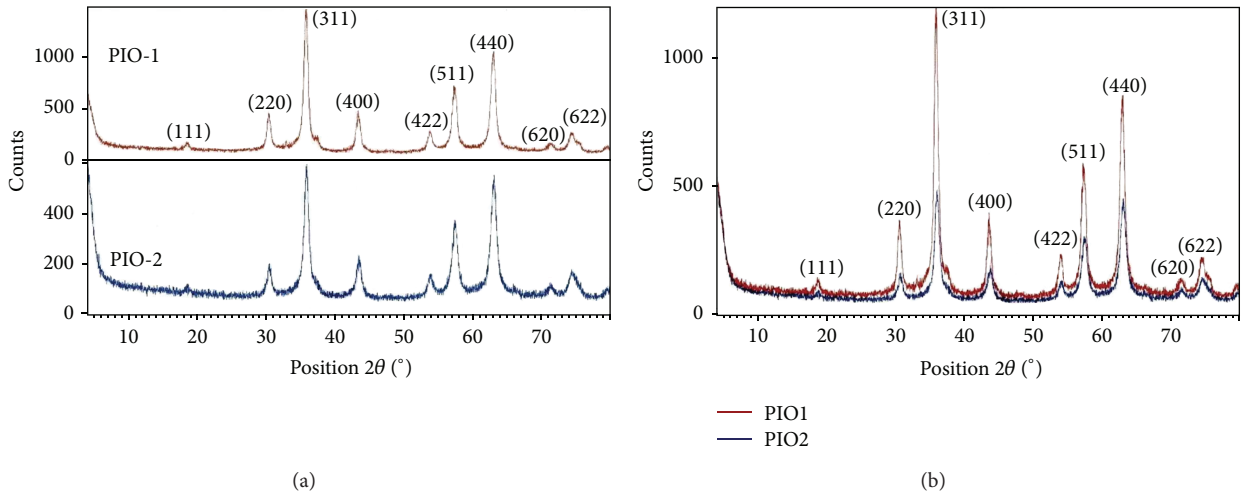

Figure 1: X-ray diffraction patterns of PIO-2 (blue, PIO-2F-left and PIO-2A-right) and PIO-1 (red, PIO-1F-left and PIO-1A-right).

Table 1: Reactant ratios and synthetic conditions.

Sample	Ferric chloride (g)	Ferrous chloride (g)	Pectin (% w/v)	Starting pH	Ending pH
PIO-1A, PIO-1F	7.8	3.0	0.3	2.5	11
PIO-2A, PIO-2F	7.8	3.0	0.5	2.5	11
PIO-3A,	7.8	3.0	0.8	2.5	11

PIO: "pectin iron oxide," A for air-dried samples, F for freeze-dried samples.

Table 2: Estimated particle size and particle size distributions.

Sample	Average particle size (nm) from pXRD	Particle size distribution (nm) from TEM
PIO-1 nanocomposites	13	5–18
PIO-2 nanocomposites	9	7–13

we can conclude that only magnetite is present in the nanocomposites.

The lattice parameters of the (311) diffraction were determined by Bragg's Law [16]:

$$d_{hkl} = \frac{a}{\sqrt{h^2 + k^2 + l^2}}. \quad (3)$$

They were found to be 8.401 and 8.384 for PIO-1 and PIO-2, respectively. The calculated values were found to be closer to the standard value of magnetite (8.391; JCPDS no. 79-0417) than those of maghemite (8.347).

3.2. Fourier-Transform Infrared Spectral Characterization (FT-IR). The FTIR spectrum of pectin (Figure 2) has a broad band at 3253 cm^{-1}, which can be attributed to the ν(O–H) stretching vibration of the hydroxyl group. The intense peak for pectin at 1750 cm^{-1} is characteristic of the carbonyl ν(C=O) stretching vibration of an ester. The bands at 1680, 1385 cm^{-1} are characteristic of asymmetric and symmetric stretching of the carboxylate group [16]. The band at 1010 cm^{-1} in pectin is assigned to the C–O bending vibration. This band is substantially reduced in intensity in the nanocomposites. The FTIR spectra of pectin and the coated magnetite nanocomposites are similar to those reported in the literature [16–18]. The presence of peaks due to pectin in the nanocomposites supports the fact that pectin actually coats the magnetite.

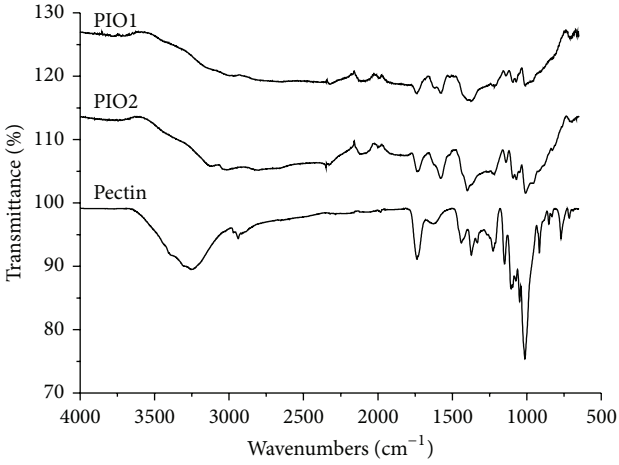

Figure 2: FT-IR spectra of pectin, PIO-1 and PIO-2 nanocomposites.

In addition to the pectin peaks seen on the FT-IR spectra of the nanocomposites, there are two new and distinct bands

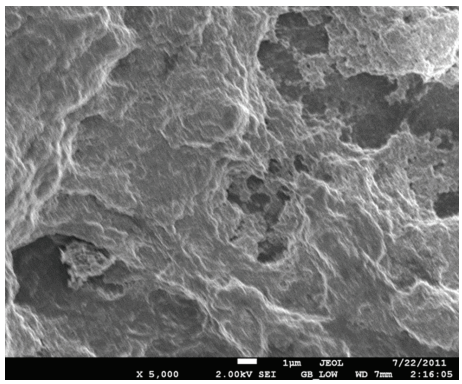

Figure 3: SEM image of PIO-2F.

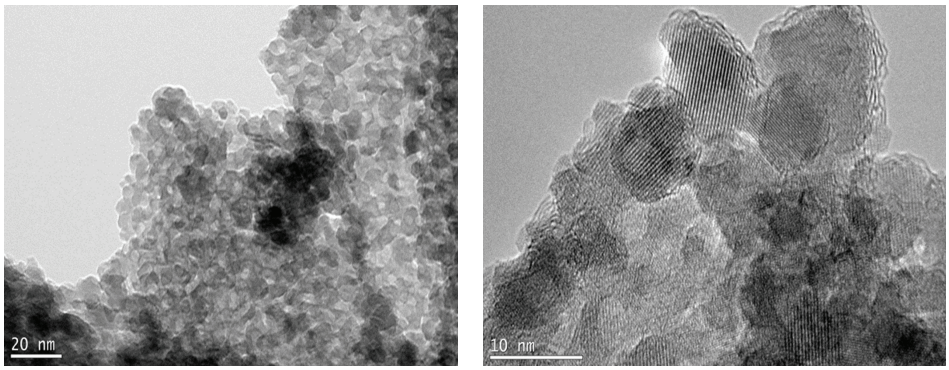

Figure 4: TEM images of PIO-2F.

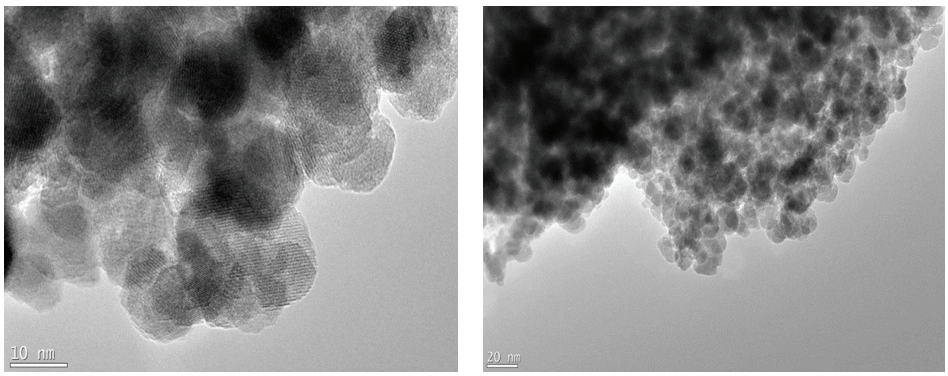

Figure 5: TEM images of PIO-1F.

at 1580 and 1408 cm^{-1}. These bands can be attributed to the symmetric and asymmetric carboxylate-metal (COO-Fe) linkage [15–19]. The wavenumber separation, Δ, between the ν_{as} (COO–) and ν_{s} (COO–) IR bands can be used to distinguish the type of the interaction between the carboxylate head and the metal atom. The Δ(1580–1408 = 172 cm^{-1}) was ascribed to bridging bidentate, where the interaction between the COO– group and the Fe atom is covalent [20, 21].

3.3. Electron Microscopy. The SEM image in Figure 3 (PIO-2F shown as an example) shows that the polymeric nature of the pectin remained intact during the synthesis. There is no agglomeration of the particles indicating that the pectin coated the magnetite nanoparticles. The estimated mean particle diameter (Table 2) measured from the TEM images is found to be consistent with the XRD results. The effect of the drying method on the nanocomposite can be seen in the TEM images, where the air-dried samples exhibited some shrinkage, observed as tearing of films (Figures 6 and 7). Figures 4 and 5 show more uniformity of pore size, shape, and distribution, suggesting less/more uniform shrinkage of the nanocomposite during freeze-drying. While many of the particles are coated in pectin (see Figure 4), nanoparticles were also clearly found on the surface of both PIO-1A and

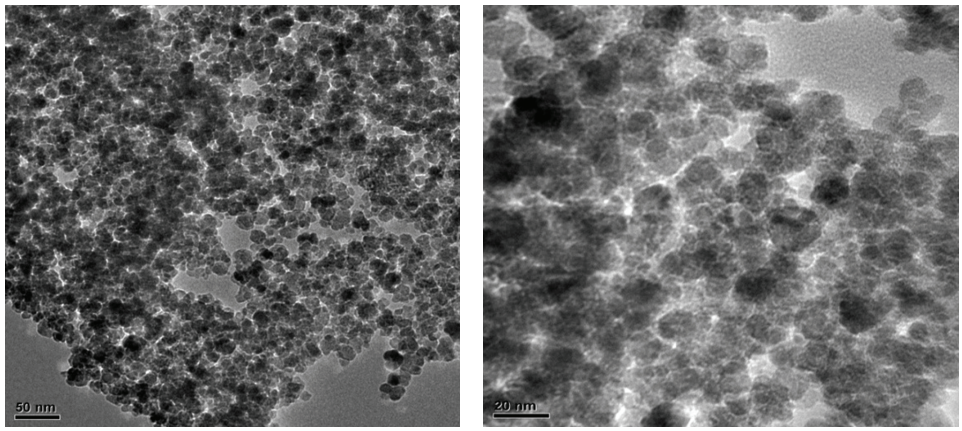

Figure 6: TEM images of PIO-2A.

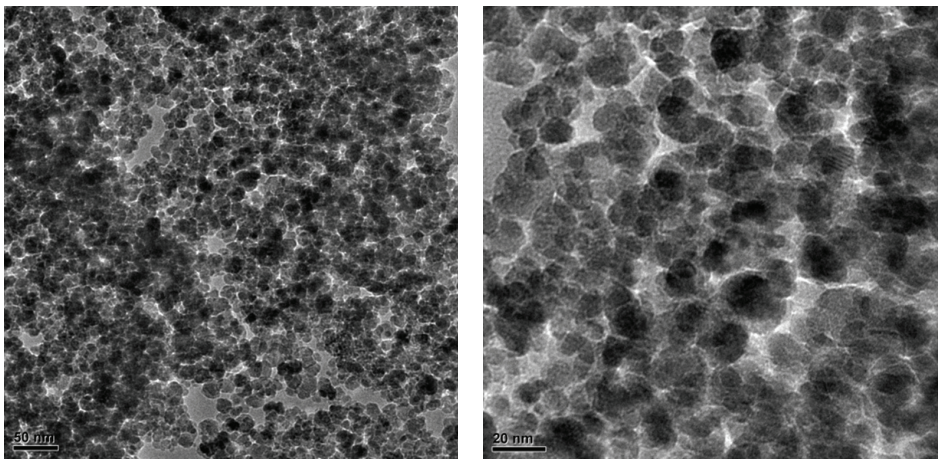

Figure 7: TEM images of PIO-1A.

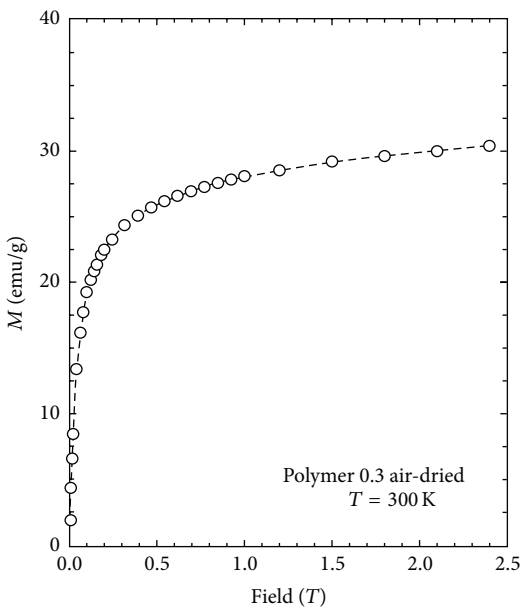

Figure 8: Magnetization curve of PIO-1A measured at 300 K.

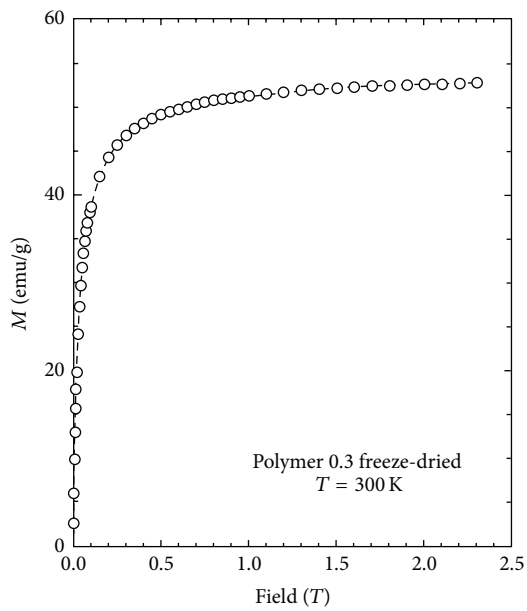

Figure 9: Magnetization curve of PIO-1F measured at 300 K.

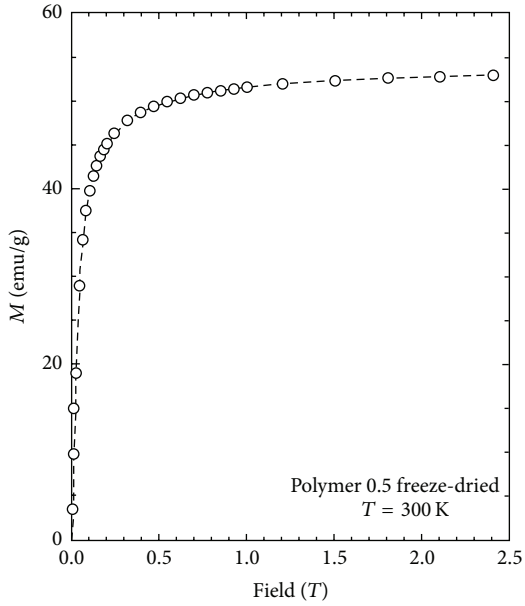

Figure 10: Magnetization curve of PIO-2F measured at 300 K.

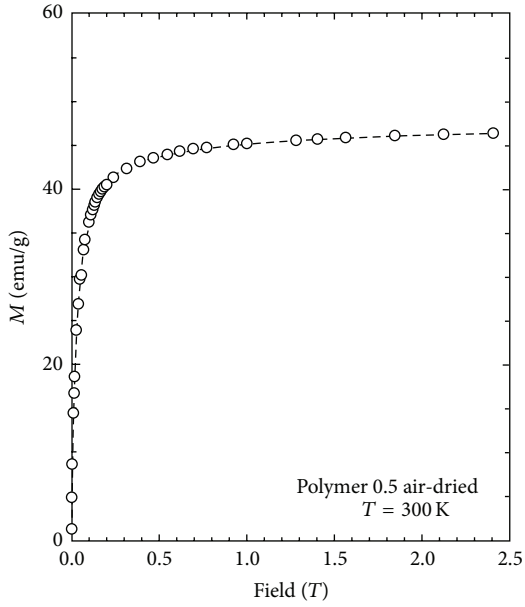

Figure 11: Magnetization curve of PIO-2A measured at 300 K.

PIO-1F. This outcome is attributed to the high magnetite to pectin ratio, especially in PIO-1A and 1F.

3.4. Magnetic Studies. The magnetic properties of nanoparticles are highly dependent on the particle size. In order to have superparamagnetic nanoparticles the nanoparticles must have a mean diameter of less than 20 nm. For superparamagnetic nanoparticles to have a high saturation magnetization, the agglomeration of these particles after synthesis must be overcome. Figures 8, 9, 10, and 11 show the magnetic susceptibility of the nanocomposites at a constant temperature of 300 K under varying magnetic fields. It is observed that the samples rise to maximum magnetisation very rapidly, and this observation is similar to that of superparamagnetic nanocomposites at room temperature reported in the literature [16, 19]. This indicates that the particles can be controlled by an external magnetic field.

Table 3: Saturation magnetization values for the nanocomposite.

Sample	Saturation magnetization (emu/g)
PIO-1A	31
PIO-1F	53
PIO-2A	46
PIO-2F	54

The interparticle distance is an important factor that affects the saturation magnetization values of magnetic nanoparticles as the strength of the magnetic moment interaction depends on the interparticle distance [10]. This is evident in the results presented in Table 3, as both PIO-1F and PIO-2F have the highest saturation magnetization values of 53 and 54 emu/g, respectively, in spite of the difference in the magnetite to pectin ratios. This can be attributed to the fact that, during the freeze-drying process, there was less shrinkage in the polymer cage hosting the nanoparticles than in the case with the air-dried particles. The air-dried nanocomposites show a drop in the saturation magnetization values; this is due to the shrinkage of the polymer host during drying, reducing the interparticle distance. This results in an increased interparticle magnetic moment interaction and a consequent decrease in the total magnetization [22, 23]. Comparing the saturation magnetization values of PIO-1A and PIO-1F, the net difference is 22 emu/g which is greater than the difference of 8 emu/g, for PIO-2A and PIO-2F. This outcome shows that the saturation magnetization does not only depend on the drying conditions but also on the reactant ratios, as PIO-1 nanocomposites have a higher magnetite to pectin ratio compared to the PIO-2 nanocomposite.

From Table 4 we see that the magnetisation values for PIO-1F and PIO-2F with pectin coating are higher than the values found in the literature for air-dried samples. There is a significant drop in magnetisation values of the air-dried nanocomposites, compared to that of pure magnetite nanoparticles; this is due to the formation of magnetic dead layer by pectin at the domain boundary wall of MNPs [16]. This drop in magnetisation is not observed in our work, especially for the freeze-dried samples.

Further work on the application of these nanoparticles to the treatment of disease is on-going, but early results using simple turbidity measurements in water medium show that these nanocomposites do not agglomerate indicating the suitability of this polymer coating for biomedical applications. Gels may also be used for producing free-standing films and coatings, opening up the possibility of fabricating more robust components.

4. Conclusion

We report the synthesis of nanocomposites of superparamagnetic magnetite nanoparticles in a pectin matrix with

Table 4: Magnetisation values for magnetite nanocomposites obtained from different precursors under different synthesis conditions.

Precursors	Synthesis method	Coating agent	Drying method	Morphology	Size (nm)	M_s (emu/g)	References
$FeCl_3{\cdot}6H_2O$, $FeCl_2{\cdot}4H_2O$, HCl	Coprecipitation with NH_4OH	Lauric acid	—	Spherical	9.4	43	[24]
$FeCl_3{\cdot}6H_2O$, $FeSO_4{\cdot}7H_2O$, OA, UA	Coprecipitation with NH_3	Pectin	Air	Spherical	250–600	32.7	[17]
$FeCl_3{\cdot}6H_2O$, $FeCl_2{\cdot}4H_2O$	Coprecipitation with NH_3	Pectin	Oven dry	Spherical	77	59.2	[18]
$FeCl_3{\cdot}6H_2O$, $FeSO_4{\cdot}7H_2O$, NaOAc	Coprecipitation with KOH	Sodium citrate	Air dry	Hexagonal	6	42.5	[25]
$Fe(NO_3)_3{\cdot}9H_2O$, $FeSO_4{\cdot}7H_2O$	Coprecipitation with NH_3	Pectin	Air dry	Spherical	50–200	46.2	[16]
$FeCl_3{\cdot}6H_2O$, $FeCl_2{\cdot}4H_2O$	Coprecipitation with NH_4OH	Pectin	Freeze dry	Cubic	5–18	53	This work
$FeCl_3{\cdot}6H_2O$, $FeCl_2{\cdot}4H_2O$	Coprecipitation with NH_4OH	Pectin	Freeze dry	Cubic	7–13	54	This work

OA: oleic acid; UA: undecylenic acid; M_s: magnetisation; NaOAc: sodium acetate.

high saturation magnetization of 53 emu/g and 54 emu/g and demonstrate the dependence of the magnetic property of these nanocomposites on the drying conditions and reactant ratios. The particle size and homogeneity were controlled by the presence of the pectin. Thus a facile in situ coprecipitation synthetic approach of magnetite-pectin nanocomposite at room temperature has been demonstrated. Freeze-drying is routinely used for the production of fruits, vegetables, and pharmaceutical products. The combination of the facile precipitation method and freeze-drying presents the possibility for producing large quantities of SPION-based composites with better control over properties. Such nanocomposites have promising biomedical and environmental applications.

Acknowledgments

Rhodes University is acknowledged for funding, and the laboratory of Professor Strydom is acknowledged for assistance with the magnetic susceptibility measurements. Dr J Botha at the high-resolution transmission microscopy centre at Nelson Mandela Metropolitan University is acknowledged for assistance with electron microscopy. One author would like to thank the University of Buea for a South Africa-Cameroon exchange visit.

References

[1] T. S. Mohammad, N. E. Mojtaba, S. E. Ali, and E. Ehsan, "Magnetite/polyvinylpyrrolidone nanocomposite: green simple fabrication and characterization," in *Proceedings of the 2nd International Conference on Chemistry and Chemical Engineering (IPCBEE '11)*, vol. 14, pp. 174–177, 2011.

[2] M. A. Garza-Navarro, V. Gonzalez, M. Hinojosa, and A. Torres-Castro, "Preparation of chitosan/magnetite polymeric-magnetic films," *Revista Mexicana de Fisica S*, vol. 57, no. 2, pp. 51–56, 2011.

[3] T. Schlorf, M. Meincke, E. Kossel, C. C. Glüer, O. Jansen, and R. Mentlein, "Biological properties of iron oxide nanoparticles for cellular and molecular magnetic resonance imaging," *International Journal of Molecular Sciences*, vol. 12, no. 1, pp. 12–23, 2011.

[4] S. R. Dave and X. Gao, "Monodisperse magnetic nanoparticles for biodetection, imaging, and drug delivery: a versatile and evolving technology," *WIREs Nanomedicine and Nanobiotechnology*, vol. 1, no. 6, pp. 583–609, 2009.

[5] Q. L. Hu, J. Wu, F. P. Chen, and J. C. Shen, "Biomimetic preparation of magnetite/chitosan nanocomposite via in situ composite method—potential use in magnetic tissue repair domain," *Chemical Research in Chinese Universities*, vol. 22, no. 6, pp. 792–796, 2006.

[6] M. Mahmoudi, A. Simchi, M. Imani, and U. O. Hafeli, "Superparamagnetic iron oxide nanoparticles with rigid cross-linked polyethylene glycol fumarate coating for application in imaging and drug delivery," *Journal of Physical Chemistry C*, vol. 113, no. 19, pp. 8124–8131, 2009.

[7] T. Yang, C. Shen, Z. Li et al., "Highly ordered self-assembly with large area of Fe_3O_4 nanoparticles and the magnetic properties," *Journal of Physical Chemistry B*, vol. 109, no. 49, pp. 23233–23236, 2005.

[8] N. Chomchoey, D. Bhongsuwan, and T. Bhongsuwan, "Magnetic properties of magnetite nanoparticles synthesized by oxidative alkaline hydrolysis of iron powder," *Kasetsart Journal: Natural Science*, vol. 44, no. 5, pp. 963–971, 2010.

[9] J. Neamtu and N. Verga, "Magnetic nanoparticles for magnetoresonance imaging and targeted drug delivery," *Digest Journal of Nanomaterials and Biostructures*, vol. 6, no. 3, pp. 969–978, 2011.

[10] J. Mazo-Zuluaga, J. Restrepo, F. Muñoz, and J. Mejía-López, "Surface anisotropy, hysteretic, and magnetic properties of magnetite nanoparticles: a simulation study," *Journal of Applied Physics*, vol. 105, pp. 123907–1123916, 2009.

[11] A. H. Lu, E. L. Salabas, and F. Schüth, "Magnetic nanoparticles: synthesis, protection, functionalization, and application," *Angewandte Chemie*, vol. 46, no. 8, pp. 1222–1244, 2007.

[12] J. Lodhia, G. Mandarano, N. J. Ferris, P. Eu, and S. F. Cowell, "Development and use of iron oxide nanoparticles (part 1): synthesis of iron oxide nanoparticles for MRI," *Biomedical Imaging and Intervention Journal*, vol. 6, no. 2, article e12, 2010.

[13] P. Tartaj, M. Del Puerto Morales, S. Veintemillas-Verdaguer, T. González-Carreño, and C. J. Serna, "The preparation of magnetic nanoparticles for applications in biomedicine," *Journal of Physics D*, vol. 36, no. 13, pp. R182–R197, 2003.

[14] P. Sriamornsak, N. Thirawong, and S. Puttipipatkhachorn, "Morphology and buoyancy of oil-entrapped calcium pectinate gel beads," *AAPS Journal*, vol. 6, no. 3, article e24, 2004.

[15] H. Iida, K. Takayanagi, T. Nakanishi, and T. Osaka, "Synthesis of Fe_3O_4 nanoparticles with various sizes and magnetic properties by controlled hydrolysis," *Journal of Colloid and Interface Science*, vol. 314, no. 1, pp. 274–280, 2007.

[16] S. Sahu and R. K. Dutta, "Novel hybrid nanostructured materials of magnetite nanoparticles and pectin," *Journal of Magnetism and Magnetic Materials*, vol. 323, no. 7, pp. 980–987, 2011.

[17] J. Dai, S. Wu, W. Jiang et al., "Facile synthesis of pectin coated Fe_3O_4 nanospheres by the sonochemical method," *Journal of Magnetism and Magnetic Materials*, vol. 331, pp. 62–66, 2013.

[18] J. L. Gong, X. Y. Wang, G. M. Zeng et al., "Copper (II) removal by pectin-iron oxide magnetic nanocomposite adsorbent," *Chemical Engineering Journal*, vol. 185-186, pp. 100–107, 2012.

[19] D. Predoi, E. Andronescu, M. Radu, M. C. Munteanu, and A. Dinischiotu, "Synthesis and characterization of bio-compatible maghemite nanoparticles," *Digest Journal of Nanomaterials and Biostructures*, vol. 5, no. 3, pp. 779–786, 2010.

[20] L. Guo, G. Liu, R. Y. Hong, and H. Z. Li, "Preparation and characterization of chitosan poly(acrylic acid) magnetic microspheres," *Marine Drugs*, vol. 8, no. 7, pp. 2212–2222, 2010.

[21] K. S. Wilson, L. A. Harris, J. D. Goff, J. S. Riffle, and J. P. Dailey, "A generalized method for magnetite nanoparticle steric stabilization utilizing block copolymers containing carboxylic acids," *European Cells and Materials*, vol. 3, no. 2, pp. 206–209, 2002.

[22] H. El Ghandoor, H. M. Zidan, M. M. H. Khalil, and M. I. M. Ismail, "Synthesis and some physical properties of magnetite (Fe_3O_4) nanoparticles," *International Journal of Electrochemical Science*, vol. 7, pp. 5734–55745, 2012.

[23] L. Zhang, R. He, and H. C. Gu, "Oleic acid coating on the monodisperse magnetite nanoparticles," *Applied Surface Science*, vol. 253, no. 5, pp. 2611–2617, 2006.

[24] J. B. Mamani, A. J. Costa-Filho, D. R. Cornejo, E. D. Vieira, and L. F. Gamarra, "Synthesis and characterization of magnetite nanoparticles coated with lauric acid," *Materials Characterization*, vol. 81, pp. 28–36, 2013.

[25] R. G. Ruiz-Moreno, A. I. Martinez, R. Castro-Rodriguez, and P. Bartolo, "Synthesis and characterization of citrate coated magnetite nanoparticles," *Journal of Superconductivity and Novel Magnetism*, vol. 26, pp. 709–712, 2013.